Journal of Magnetism and Magnetic Materials 401 (2016) 684–694

Contents lists available at ScienceDirect

Journal of Magnetism and Magnetic Materials

journal homepage: www.elsevier.com/locate/jmmm

Spin-polarization in filled-skutterudites $LaFe_4Pn_{12}$ (Pn=P, As and Sb)

A.H. Reshak [a,b,*]

[a] New Technologies-Research Centre, University of West Bohemia, Univerzitni 8, 306 14 Pilsen, Czech Republic
[b] Center of Excellence Geopolymer and Green Technology, School of Material Engineering, University Malaysia Perlis, 01007 Kangar, Perlis, Malaysia

A R T I C L E I N F O

Article history:
Received 9 May 2015
Received in revised form
12 August 2015
Accepted 26 October 2015
Available online 28 October 2015

PACS:
71.15.Mb
71.20.-b

Keywords:
Filled skutterudite
Spin polarization
Electronic band structure
Fermi surface
Electronic charge density distribution

A B S T R A C T

We have performed spin-polarized calculation for the electronic band structure, density of states, Fermi surface and the space electronic charge density distribution for the filled-skutterudites $LaFe_4Pn_{12}$ (Pn=P, As and Sb) compounds. It has been noticed that for both $LaFe_4P_{12}$ and $LaFe_4As_{12}$ there are two bands cross Fermi level (E_F) for the spin-up and spin-down states, while for $LaFe_4Sb_{12}$ there is only one band cross E_F for the spin-up state and three bands cross E_F for the spin-down state. As the partial DOS of La-s, d, Fe-s/p/d and Pn-s/p/d coincide Fermi level at nonzero value, it reveals that the electrons of these orbitals contribute in the conduction process. The calculated values of the density of the states at Fermi level $N(E_F)$ and the associated electronic specific heat coefficient (γ) for the spin-up/down states are decreases with substituting P→As→Sb. The bonds nature and the interactions between the atoms for the spin-up/down configurations were investigated in (1 0 0) and (1 0 1) crystallographic planes.

1. Introduction

Due to their interesting physical and chemical properties, the filled skutterudite compounds have attracted much attention as potential candidates. It has been demonstrated that the filled skutterudite compounds are promising materials for electrical, magnetic and thermoelectric applications [1] due to their high carrier mobility, low lattice thermal conductivity and low electrical resistivity [1–3]. Much more interesting phenomena have been observed in the filled skutterudite compounds, for instance semiconductivity [4,5], superconductivity [6–8], magnetic order [9–13], metal-insulator transition material [14] and valence fluctuation and heavy fermion behavior [15–17]. Moreover, the filled skutterudite compounds $LaFe_4Pn_{12}$ (Pn=P, As and Sb) exhibit phonon-glass electron-crystals which make these compounds as promising materials for thermoelectric applications [18–20]. The La-based filled skutterudite phosphide, arsenide and antimonide [21,22] are very important members of the filled skutterudite compounds. Therefore, several researchers have performed experimental and theoretical investigation on this group in order to understand the functionality of these materials. Recently Pulikkotil et al. [20] have performed first-principles calculations within local density approximation (LDA) to clarify the influence of $FeSb_6$ octahedral deformations on the structural and electronic structure properties of $LaFe_4Sb_{12}$. It has been found that octahedral tilting correlate with the band dispersions and hence the band masses [20].

The band structure and Fermi surface of $LaFe_4Pn_{12}$ (Pn=P, As and Sb) compounds were investigated theoretically within the density functional theory [23]. Furthermore, using the full potential linear augmented plane wave (FPLAPW) method within the local density approximation (LDA), Takegahara and Harima [24] investigated the band structure of simple cubic $LaRu_4P_{12}$ and the orthorhombic $LaFe_4P_{12}$ compounds. The Fermi surface and the hybridization between La-f orbital and P-p states were also investigated. An *ab initio* calculation using LDA to investigate the structural and elastic properties of $LaFe_4Pn_{12}$ (Pn=P, As and Sb) compounds were reported by Hachemaoui et al. [25]. The density of states near Fermi level and the corresponding thermoelectric properties of $LaFe_4Sb_{12}$ and $CeFe_4Sb_{12}$ compounds were investigated using tight-binding linear muffin-tin orbital (TB-LMTO) and full potential linear augmented plane wave (FPLAPW) methods [26]

From above it is clear that there exists a number of band structure calculations for $LaFe_4Pn_{12}$ (Pn=P, As and Sb) compounds using different methods within local density approximation (LDA) and generalized gradient approximation (GGA) as exchange and

* Corresponding author at: New Technologies-Research Centre, University of West Bohemia, Univerzitni 8, 306 14 Pilsen, Czech Republic.
E-mail address: maalidph@yahoo.co.uk

http://dx.doi.org/10.1016/j.jmmm.2015.10.099
0304-8853/

correlation potentials. It is well know that for the highly correlated compounds, LDA and GGA are known to fail to give the correct ground state. In these systems, the electrons are highly localized. The Coulomb repulsion between the electrons in open shells should be taken into account [27]. Therefore, this motivates us to address ourselves for a comprehensive theoretical calculation using the all-electron full potential linear augmented plane wave plus the local orbitals (FPLAPW+lo) method within the recently modified Becke–Johnson potential (mBJ) [28], to investigate the influence of substituting P→As→Sb on the electronic band structure, density of states, Fermi surface and the electronic charge distributions. The modified Becke–Johnson potential allows the calculation with accuracy similar to the very expensive GW calculations [28]. It is a local approximation to an atomic "exact-exchange" potential and a screening term. To the best of our knowledge there is dearth of spin polarizing calculation for the $LaFe_4Pn_{12}$ (Pn=P, As and Sb) compounds therefore, we have calculated the spin polarized electronic band structure, electronic charge distribution, total and the angular momentum resolved projected density of states and Fermi surface of these compounds meanwhile we have investigated the influence of substituting P→As→Sb on these properties in the presence of the spin polarization. The FPLAPW+lo method has proven to be one of the accurate methods for the computation of the electronic structure of solids within density functional theory (DFT) [29–33].

2. Details of calculations

The electronic and magnetic properties of the filled-skutterudites $LaFe_4Pn_{12}$ (Pn=P, As and Sb) compounds are calculated using the all-electron full potential linear augmented plane wave plus local orbitals (FPLAPW+lo) method accomplished by using the WIEN2k code [34]. It is well known that the electronic properties of any compound are strongly depend on the configuration of the electronic structure, thus it is essential to investigate the electronic structure. $LaFe_4Pn_{12}$ (Pn=P, As and Sb) compounds crystallized in cubic structure, the space group is Im−3. In the unit cell, La atom is situated at 2a (0.0, 0.0, 0.0), Fe at 8c (0.25, 0.25, 0.25) and X at 24 g (0.0, u, v) [21,22]. The lattice constant a and the two internal free parameters u and v were optimized by minimizing the total energy. The optimization is achieved using the local density approximation (LDA) [35]. These values are listed in Table 1 along with the bulk modulus B in (GPa) and its pressure derivative B', in comparison with the experimental data and the previous results [22,23,25,36–38]. In order to achieve energy eigenvalues convergence, the wave functions in the interstitial region are expanded in terms of plane waves with a cut-off of $K_{MAX}=8/R_{MT}$. Self-consistency was achieved using 800 $\vec{k}$ points in the irreducible Brillouin zone (IBZ). The spin-polarized electronic band structure and the related properties were calculated within 5000 $\vec{k}$ points in IBZ using the recently modified Becke–Johnson potential (mBJ) [28]. The self-consistent calculations were converged since the total energy of the system was stable within 10^{-5} Ry.

3. Results and discussion

3.1. Spin polarized electronic band structure and density of states

Using mBJ approach the electronic band structure of $LaFe_4Pn_{12}$ (Pn=P, As and Sb) compounds are obtained for spin-up and spin-down electrons as shown in Fig. 1(a)–(f). We set the zero-point of energy at Fermi level (E_F). It has been found that the spin-polarization show significant influence on the bands dispersion. Also moving from P to As to Sb cause significant influence on the bands dispersion mainly the dispersionless bands below E_F which show large peak at E_F in the density of states as illustrated in Figs. 2(a), 3(a) and 4(a). That is attributed to the fact that moving from P→As→Sb lead to increase the interatomic distances which cause to push up electronic energies on the neighboring atoms. Also it has been noticed that for both of $LaFe_4P_{12}$ and $LaFe_4As_{12}$ there are two bands cut E_F for the spin-up and spin-down cases, while for $LaFe_4Sb_{12}$ there is only one band cuts E_F for the spin-up case and three bands cut E_F for the spin-down case. To confirm the influence of substituting P→As→Sb on the spin-up/down configurations in the electron structure, we have calculated the spin-up and spin-down total and partial density of states as shown in Figs. 2–4. We would like to mention that the density of states exhibits the distribution of the electronic state as a function of energy. The area under each curve for each individual energy interval equals to the number of allowed electronic states in the particular interval. The spin polarization cause to reduce the value of the density of states at Fermi level $N(E_F)$when we move from P→As→Sb for both spin-up and spin-down. Also a clear reduction can be seen in the associated electronic specific heat coefficient (γ) which can be determined by using the expression $\gamma=\frac{1}{3}\pi^2 N(E_F)k_B^2$, where k_B is the Boltzmann constant. The calculated values of $N(E_F)$ and γ for $LaFe_4Pn_{12}$ (Pn=P, As and Sb) compounds are listed in Table 2. We should emphasize that the electro-negativity of P, As and Sb atoms are 2.19, 2.18 and 2.05, respectively according to the Pauling scale. Therefore, due to the small electro-negativity differences between P, As and Sb, no more peaks will be introduced in the density of states when we move from P→As→Sb. The desperation of the PDOS helps to identify the angular momentum characters of the various structures. It is clear that La-s, Fe-s/p and Pn-s/p states are contributing along the whole energy range for both spin-up and spin-down configurations. While the contribution of Fe-d state is confined in two regions (−6.0 upto E_F) eV and (0.1 and above), La-d contribute from 1.5 eV and above whereas La-f concentrated around 3.0 eV, and L-d exhibit main contribution above E_F. It is clear that in $LaFe_4P_{12}$ compound the La-p state shows very shape rise around −16.5 eV for spin-up/down states, a significant reduction occurs in La-p state for the spin-down state when we

Table 1
The calculated lattice constant, the free internal parameters u and v and the bulk modulus B in (GPa) and its pressure derivative $B'$of $LaFe_4Pn_{12}$ (Pn=P, As and Sb) in comparison with the experimental data and the previous theoretical results.

	$LaFe_4P_{12}$	$LaFe_4As_{12}$	$LaFe_4Sb_{12}$
a (Å)	7.8315*	8.3251*	9.1392*
	7.724[a]	8.179[a]	8.963[a]
	7.8316[b] (Exp.)	8.3252[c] (Exp.)	9.1392[d] (Exp.)
	7.8217[f]	8.3252[f]	9.1487[e] (Exp.)
			9.1395[f]
u	0.3530*	0.3453*	0.3365*
	0.3527[a]	0.3418[a]	0.3344[a]
	0.3539[b] (Exp.)	0.34556[c](Exp.)	0.33696[d](Exp.)
v	0.1511*	0.15521*	0.1610*
	0.1543[a]	0.15667[a]	0.1612[a]
	0.1504[b] (Exp.)	0.15474[c](Exp.)	0.16042[d](Exp.)
B	160.2*	145.7*	104.5*
	177.11[a]	152.09[a]	115.82[a]
			88.9[e] (Exp.)
			101.4[e] (calc.)
B'	3.60*	3.1*	2.98*
	4.21[a]	4.03[a]	3.49[a]

[a] Ref. [25]
[b] Ref. [22]
[c] Ref. [36]
[d] Ref. [37]
[e] Ref. [38]
[f] Ref. [23]

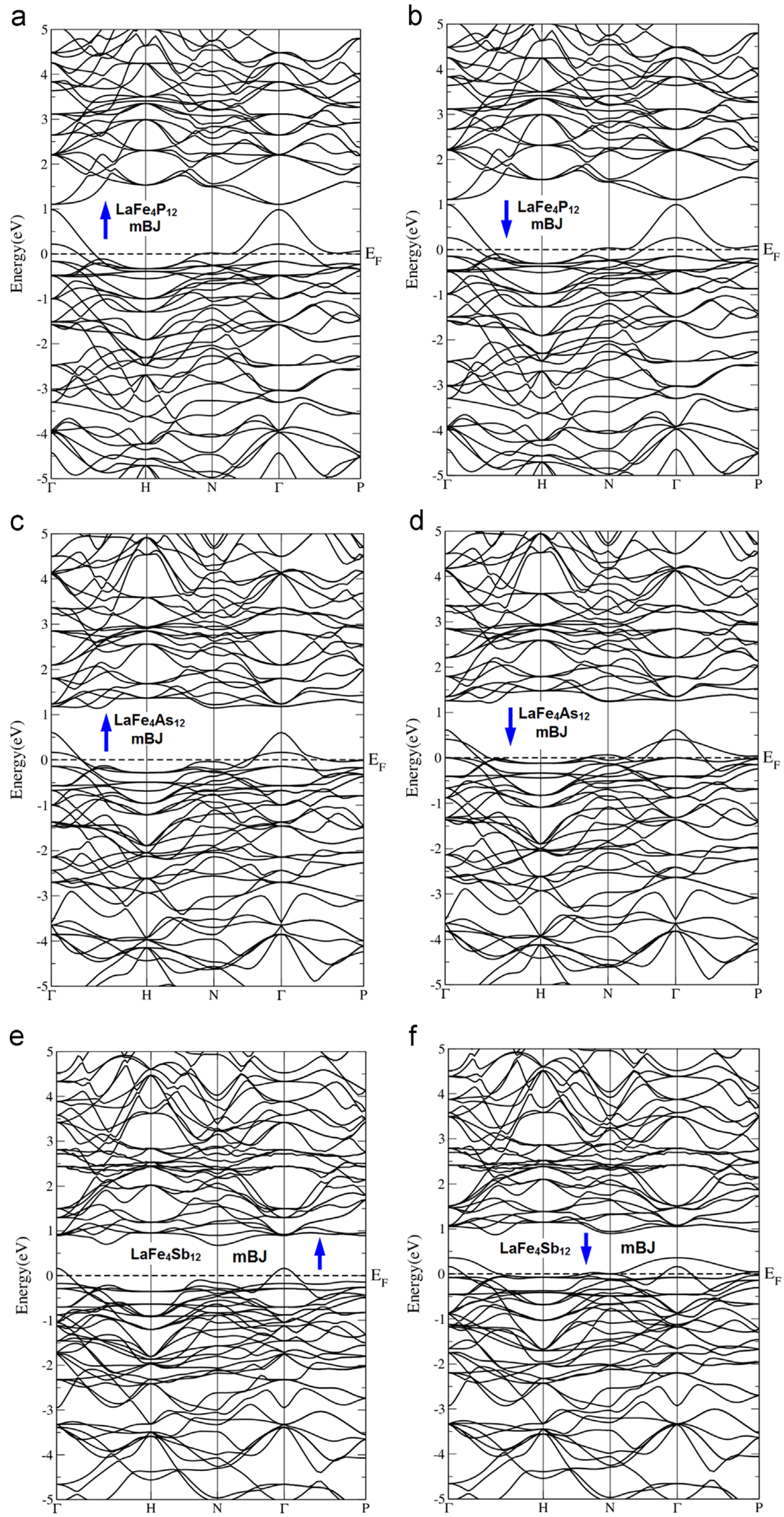

Fig. 1. : The spin-polarized electronic band structure of $LaFe_4Pn_{12}$ (Pn=P, As and Sb) compounds using mBJ approach; (a) spin-up $LaFe_4P_{12}$; (b) spin-down $LaFe_4P_{12}$; (c) spin-up $LaFe_4As_{12}$; (d) spin-down $LaFe_4As_{12}$; (e) spin-up $LaFe_4Sb_{12}$; (f) spin-down $LaFe_4Sb_{12}$.

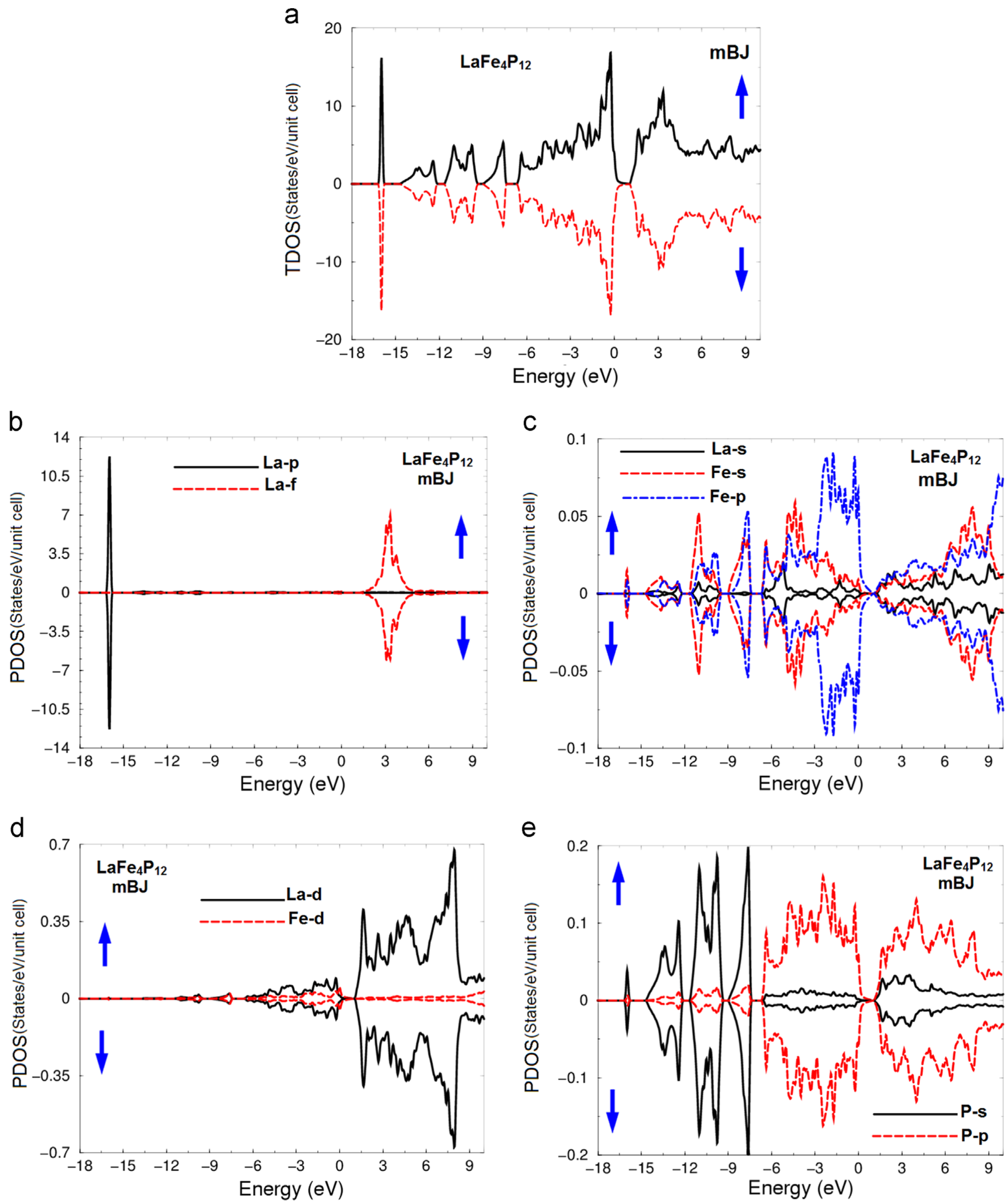

Fig. 2. : The spin-polarized total and partial density of states of $LaFe_4P_{12}$ compound using mBJ approach; (a) Total DOS spin-up/down of $LaFe_4P_{12}$; (b) PDOS spin-up/down of La-p/f states; (c) PDOS spin-up/down of La-s, Fe-s/p states; (d) PDOS spin-up/down of La-d and Fe-d states; (e) PDOS spin-up/down of P-s/p states.

substitute P by As (Figs. 2(b) and 3(b)), while it vanishes form the spin-down state of $LaFe_4Sb_{12}$ (Fig.4(b)). Since the partial DOS of La-s,d, Fe-s/p/d and *Pn*-s/p/d (Figs. 2(c)–(e), 3(c)–(e) and 4(c)–(e)) coincide E_F at nonzero value, it reveals that the electrons of these orbitals contribute in the conduction process.

From the PDOS it has been noticed that for $LaFe_4P_{12}$ at around −17.5 eV the Fe-s state hybridized with Fe-p state for spin-up and down (Fig. 2(c)), moving from P→As→Sb cause to reduce this hybridization for spin-up and vanish for the spin-down case (Figs. 3(c) and 4(c)). In the structure between −15.0 and −12.0 eV, the La-s state of $LaFe_4P_{12}$ hybridized with Fe-s/p states at around −12.0 eV (Fig. 2(c)), moving from P→As cause to shift this structure towards higher energies by around 1.0 eV and La-s hybridized with Fe-s/p at around 13.0 eV (Fig. 3(c)). Whereas moving from As→Sb cause further shift to this structure towards higher energies by around 1.0 eV leads to merge it with the next structure and leads to vanish the hybridization between La-s and Fe-s (Fig. 4(c)). For the three compounds La-s hybridized with Fe-s/p at around −5.0 and 3.0 eV (Figs. 2(c), 3(c) and 4(c)). Substituting P by As push La-s to hybridized with Fe-s/p at around 6.0 eV and with Fe-p between 6.0 and 9.0 eV (Fig. 3(c)), while moving from As to Sb push La-s to hybridized with Fe-p only between 6.0 and 7.0 eV

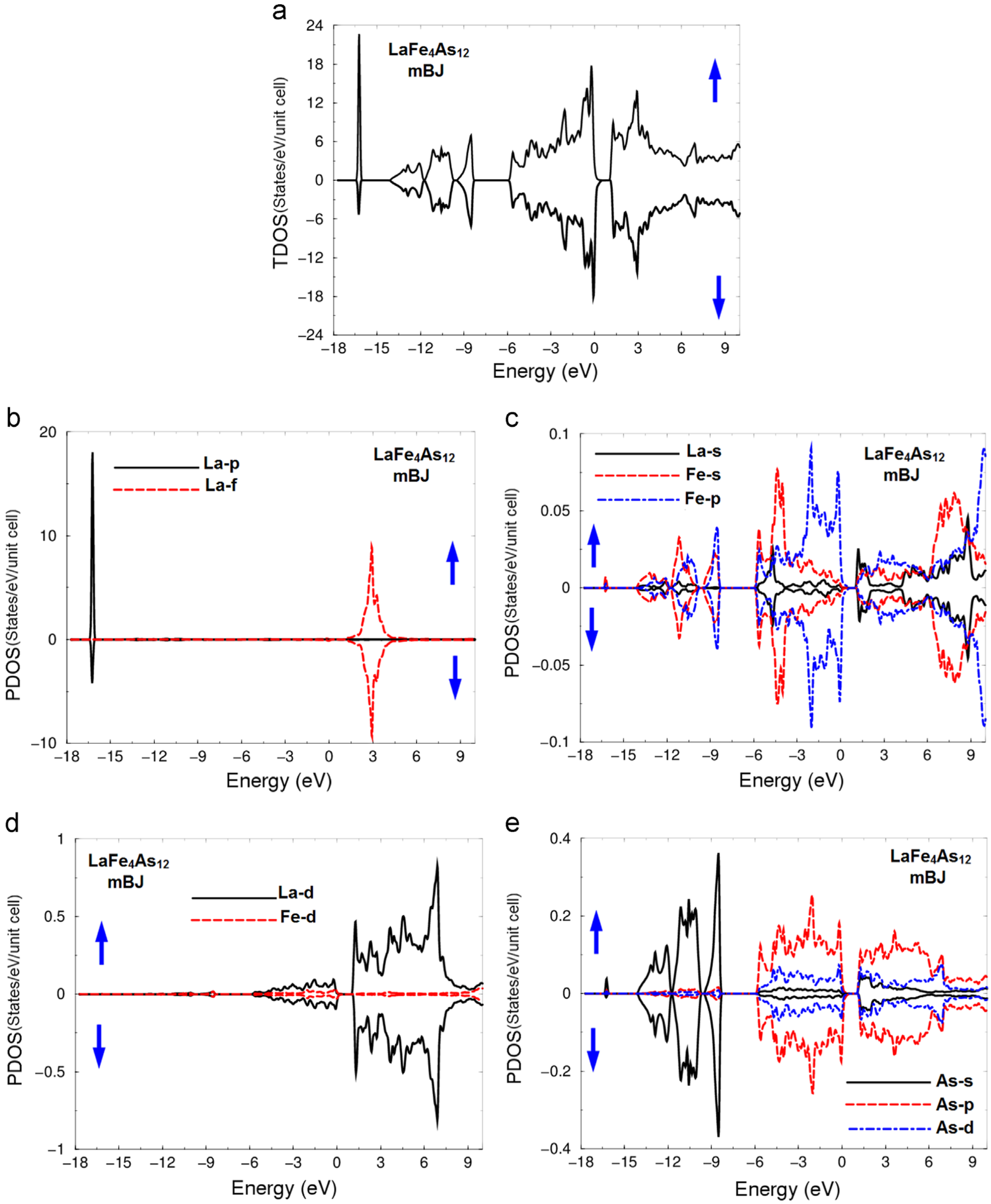

Fig. 3. **:** The spin-polarized total and partial density of states of $LaFe_4As_{12}$ compound using mBJ approach; (a) Total DOS spin-up/down of $LaFe_4As_{12}$; (b) PDOS spin-up/down of La-p/f states; (c) PDOS spin-up/down of La-s, Fe-s/p states; (d) PDOS spin-up/down of La-d and Fe-d states; (e) PDOS spin-up/down of As-s/p/d states.

(Fig. 4(c)). The La-s state hybridized with *Pn*-p between 14.0 and −9.0 eV for $LaFe_4P_{12}$ and $LaFe_4As_{12}$ and between −12.0 and 9.0 eV for $LaFe_4Sb_{12}$ (Figs. 2(c), 3(c) and 4(c)). Whereas La-s state hybridized with *Pn*-s state from −6.0 eV and above for $LaFe_4Pn_{12}$ compounds (Figs. 2(c), 3(c) and 4(c)). The La-d state hybridized with *Pn*-s state in the energy region between −7.0 and 0.0 eV for $LaFe_4P_{12}$ (Fig. 2(d)), −6.0 and 0.0 eV for $LaFe_4As_{12}$ (Fig. 3(d)) and between −5.0 and 0.0 eV for $LaFe_4Sb_{12}$ (Fig. 4(d)). Finally, the La-f state hybridized with *Pn*-s/p/d states at around 1.5 eV (Figs. 2(b), 3(b) and 4(b)).

The spin magnetic moments are calculated for the atom resolved within the muffin-tin spheres as well as in the interstitial sites as shown in Table 3. The calculated spin magnetic moments are in accordance with Slater–Pauling rule. Calculation shows that the magnetic moment of Fe sphere is the largest. As it has been mentioned above substituting P by As and As by Sb lead to increase the interatomic distances, and the increase of interatomic distances of La-Fe is larger than La-*Pn*. The increase in the interatomic distances pushes up electronic energies on the neighboring atoms. In order to clarify this we have investigated the valence electron charge density distribution in two different crystallographic planes as shown in Fig. 5. Form the

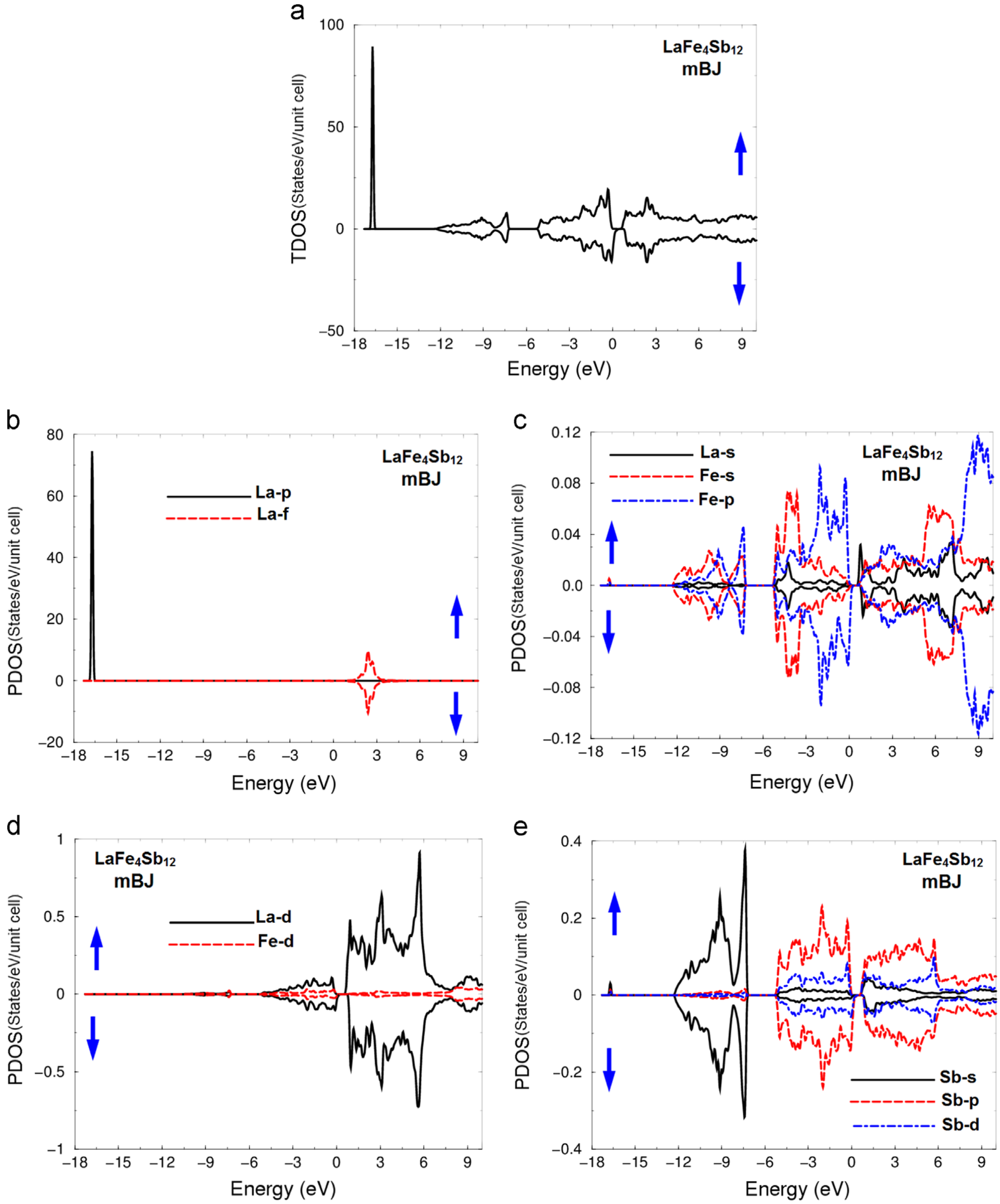

Fig. 4. **:** The spin-polarized total and partial density of states of $LaFe_4Sb_{12}$ compound using mBJ approach; (a) Total DOS spin-up/down of $LaFe_4Sb_{12}$; (b) PDOS spin-up/down of La-p/f states; (c) PDOS spin-up/down of La-s, Fe-s/p states; (d) PDOS spin-up/down of La-d and Fe-d states; (e) PDOS spin-up/down of Sb-s/p/d states.

Table 2
Calculated spin-up/down density of states at Fermi lever $N(E_F)$ for $LaFe_4Pn_{12}$ (Pn=P, As and Sb) along with the calculated electronic specific heat coefficient (γ).

Compound	$N(E_F)$ (states/Ry/cell)		γ (mJ/mole K^2)	
	Spin-up	Spin-down	Spin-up	Spin-down
$LaFe_4P_{12}$	1.20	1.04	0.21	0.18
$LaFe_4As_{12}$	0.09	0.27	0.02	0.05
$LaFe_4Sb_{12}$	0.02	0.19	0.001	0.03

Table 3
Total and local magnetic moment in $LaFe_4Pn_{12}$ (Pn=P, As and Sb).

	M^{total} (μ_B)	$m^{interstitial}$ (μ_B)	m^{La} (μ_B)	m^{Fe} (μ_B)	m^{X} (μ_B)
$LaFe_4P_{12}$	47.985	20.589	0.604	3.172	1.174
$LaFe_4As_{12}$	48.037	18.939	0.575	2.944	1.395
$LaFe_4Sb_{12}$	48.055	20.793	0.543	3.014	1.221

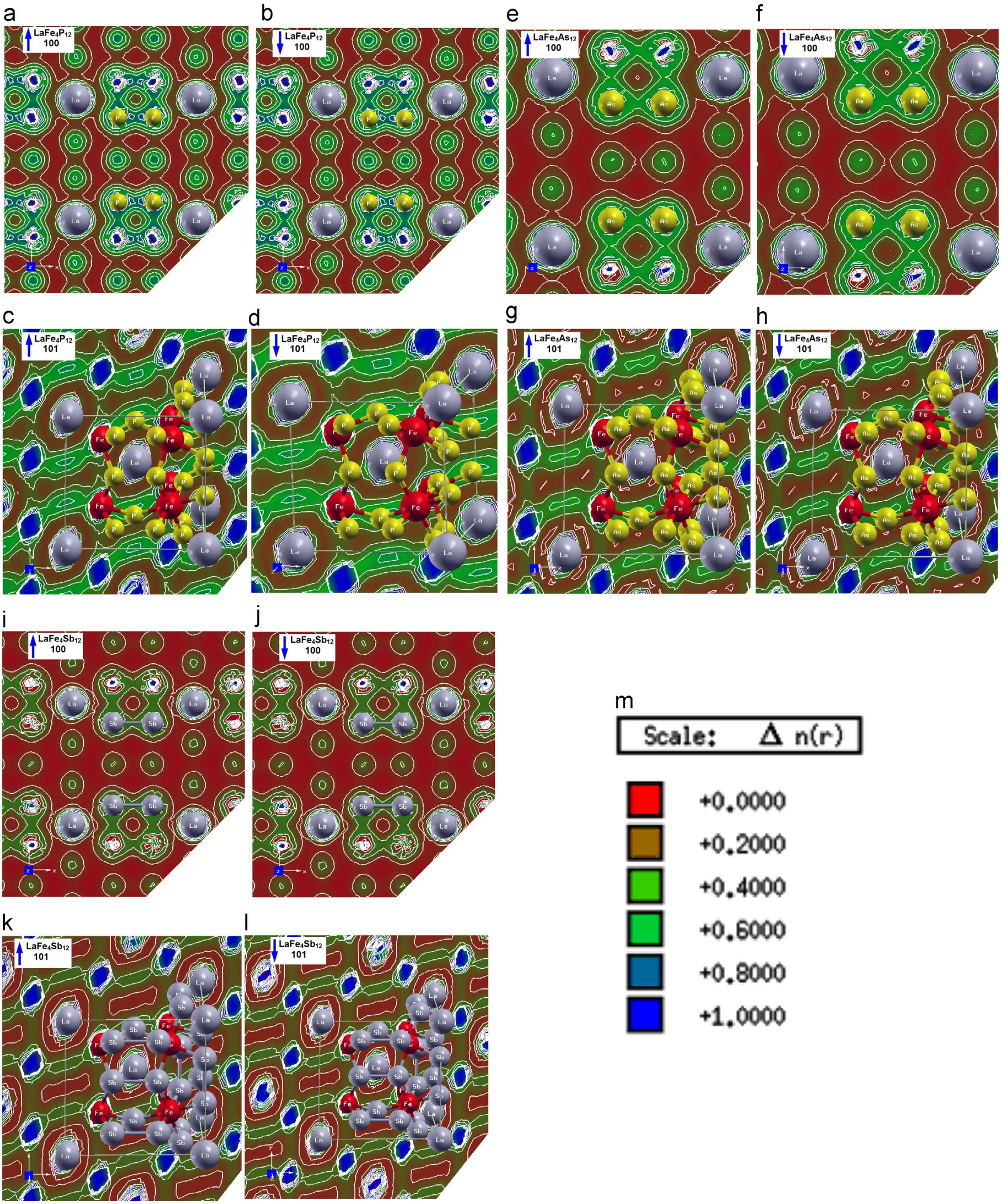

Fig. 5. : (a–l) Calculated spin-polarized electronic charge density dispersion of $LaFe_4Pn_{12}$ (Pn=P, As and Sb) compounds using mBJ approach for two crystallographic planes (1 0 0) and (1 0 1).

crystallographic plane (1 0 0) of $LaFe_4P_{12}$ compound we can see only two types of atoms namely La and P atoms. The La atoms form an ionic bonding, while P atom exhibit mainly ionic and partially covalent bonding for both spin-up/down configurations. Seeking deep investigation we have calculated the electronic charge density in (1 0 1) crystallographic plane which exhibit the

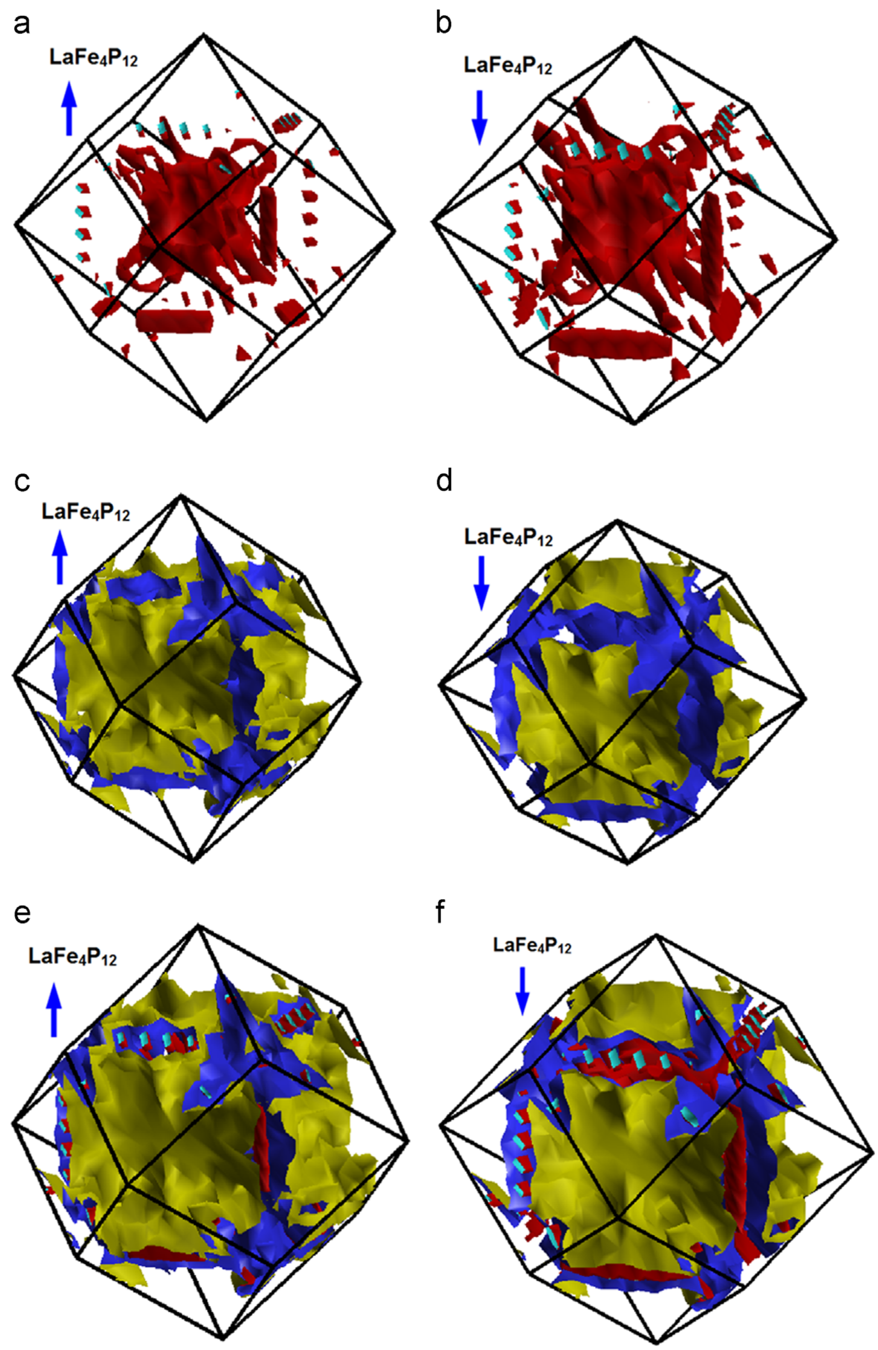

Fig. 6. : The spin-polarized Fermi surface of $LaFe_4P_{12}$ compound using mBJ approach; (a) Band # 63 spin-up; (b) Band # 63 spin-down; (c) Band # 64 spin-up; (d) Band # 64 spin-down; (e) Total spin-up; (f) Total spin-down.

three types of atoms in which the Fe atom form mainly ionic and partially covalent bonding. Substituting P by As lead to increase the atomic radius and the electro-negativity, whereas substituting As by Sb cause to perturbs the contours around La atoms lead to push La contours towards the nearest Sb atom.

The spin-up and spin-down Fermi surface of $LaFe_4Pn_{12}$ (Pn=P, As and Sb) compounds were calculated and presented in Figs. 6–8. As it is clear from the calculated electronic band structure that there are some bands cross E_F for both spin-up/down configurations. Fig. 6(a) and (b) shows the Fermi surface formed by band # 63 of spin-up/down. The observed Fermi surface consists of empty areas that represent the holes and shaded areas corresponding to the electrons. Therefore, the Fermi surface formed by band # 63 in spin-down case contains more electrons than holes on the contrary of the spin-up case. While band # 64 show almost equivalent contributions (Fig. 6(c) and (d)). The total shape of Fermi surface is illustrated in Fig. 6(e) and (f). Moving from P to As also show that two bands cross E_F, the spin-down configuration show that these two bands consist of more electrons than holes as shown in Fig. 7 (a)–(f). Which confirmed by the total shape of the Fermi surface presented in Fig. 7(e) and (f). $LaFe_4Sb_{12}$ show that there is only one band cross E_F for the spin-up configuration while three bands cross E_F for the spin-down configuration (Fig. 8(a)–(f)). It is clear that the spin-up Fermi surface is mainly formed by holes, while the spin-down Fermi surface formed by mixture of holes and more electrons. It has been noticed that in all cases the spin-down

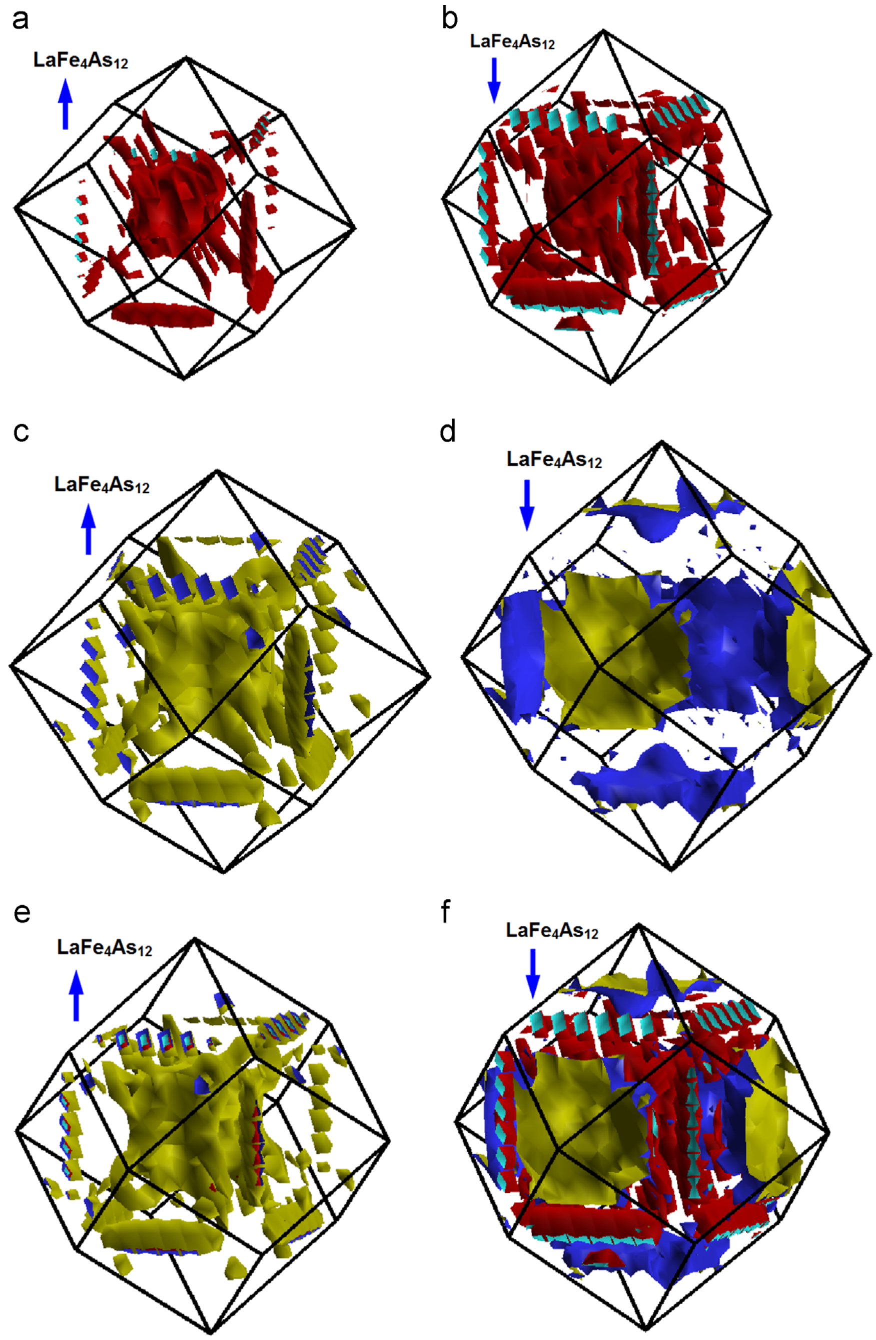

Fig. 7. **:** The spin-polarized Fermi surface of $LaFe_4As_{12}$ compound using mBJ approach; (a) Band # 123 spin-up; (b) Band # 123 spin-down; (c) Band # 124 spin-up; (d) Band # 124 spin-down; (e) Total spin-up; (f) Total spin-down.

electrons have a larger value at E_F therefore, the spin-down Fermi surface consist of more shaded areas. These electrons have more contribution in the conduction process than the spin-up electrons. Therefore, we expected that these materials are promising candidates for thermoelectric applications.

4. Conclusions

Using the all-electron full potential linear augmented plane wave plus local orbitals (FPLAPW+lo) method within the recently modified Becke–Johnson potential, we have performed spin polarized calculation for the electronic band structure, density of states, electronic charge density distribution and the Fermi surface. The lattice constant *a* and the two internal free parameters *u* and *v* were optimized by minimizing the total energy. The optimization is achieved using the local density approximation (LDA). The results show good agreement with the experimental data and the previous theoretical results. The partial density of states exhibit that La-s state hybridized with Fe-s/p states and with *Pn*-s/p states. Also it has been found that La-d state hybridized with *Pn*-s state while La-f state hybridized with *Pn*-s/p/d states. It is clear that in $LaFe_4P_{12}$ compound the La-p state show very shape rise around −17.5 eV for spin-up/down states, a significant reduction occurs in La-p state for the spin-down state when we substitute P by As, while it is vanishes form the spin-down state of $LaFe_4Sb_{12}$. It

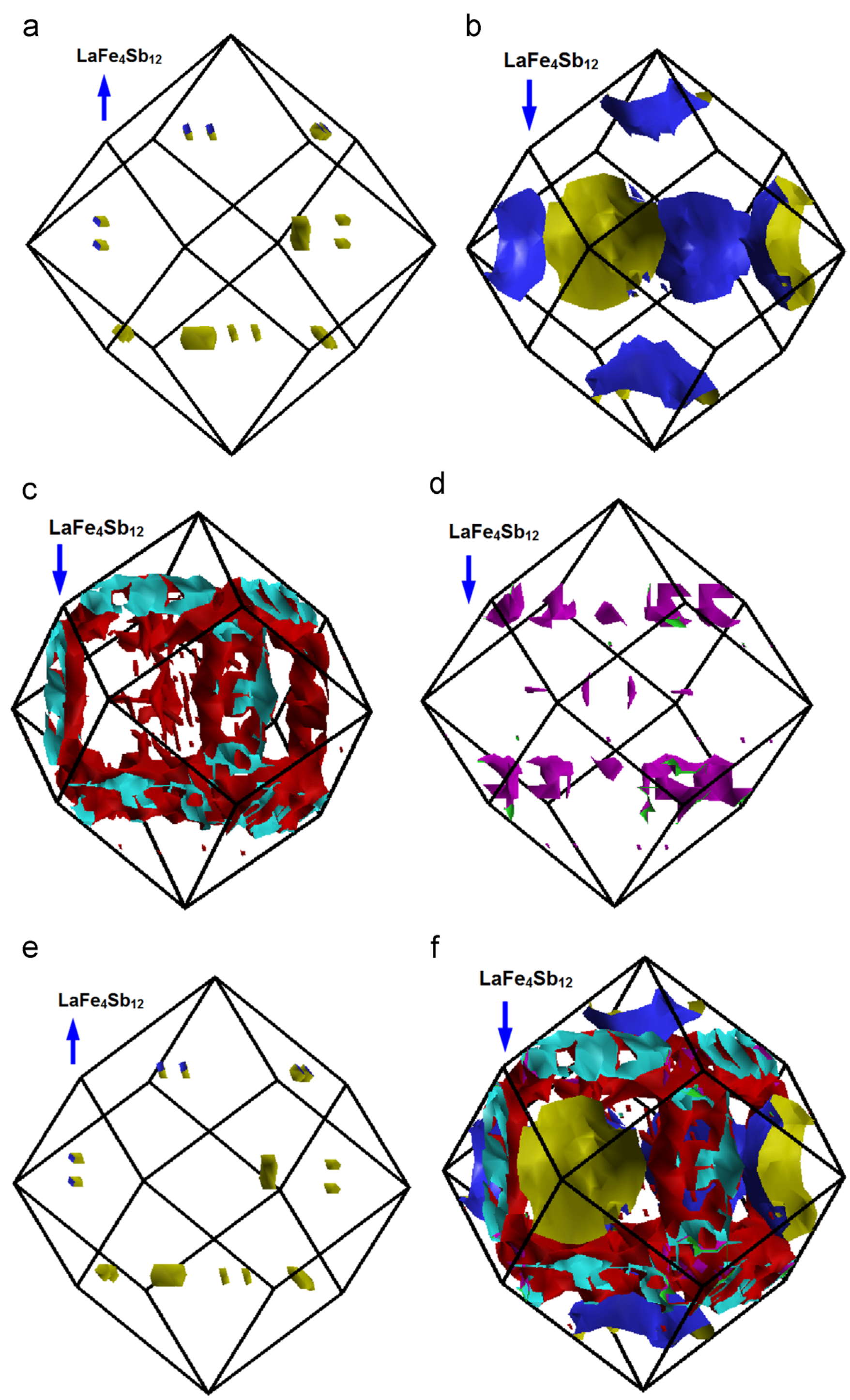

Fig. 8. : The spin-polarized Fermi surface of $LaFe_4Sb_{12}$ compound using mBJ approach; (a) Band # 124 spin-up; (b) Band # 124 spin-down; (c) Band # 123 spin-down; (d) Band # 122 spin-down; (e) Total spin-up; (f) Total spin-down.

has been noticed that the spin polarization cause to reduce the value of the density of states at Fermi level $N(E_F)$ when we move from P→As→Sb for both spin-up and spin-down. Also a clear reduction can be seen in the associated electronic specific heat coefficient (γ). The values of $N(E_F)$ and γ confirm the metallicity of the investigated materials. The spin-up Fermi surface is mainly formed by holes, while the spin-down Fermi surface formed by mixture of holes and more electrons. In all cases the spin-down electrons have a larger value at E_F. These electrons have more contribution in the conduction process than that of the spin-up electrons. Therefore, we expected that these materials are promising candidates for thermoelectric applications.

Acknowledgments

The result was developed within the CENTEM project, reg. no. CZ.1.05/2.1.00/03.0088, cofunded by the ERDF as part of the Ministry of Education, Youth and Sports OP RDI programme and in the follow-up sustainability stage, supported through CENTEM PLUS (LO1402) by financial means from the Ministry of Education, Youth and Sports under the National Sustainability Programme I. Computational resources were provided by MetaCentrum (LM2010005) and CERIT-SC (CZ.1.05/3.2.00/08.0144) infrastructures.

References

[1] G.D. Mahan, H. Ehreinreich, F. Spaepen (Eds.), Solid State Physics, 51, Academic Press, New York, 1998, p. 81.
[2] B.C. Sales, D. Madrus, B.C. Chakoumakos, V. Keppens, J.R. Thompson, Phys. Rev. B 56 (1997) 15081.
[3] G.S. Nolas, J.L. Cohn, G.A. Slack, Phys. Rev. B 58 (1998) 164.
[4] G.P. Meisner, M.S. Torikachvili, K.N. Yang, M.B. Maple, R.P. Guertin, J. Appl. Phys. 57 (1985) 3073.
[5] I. Shirotani, T. Uchiumi, C. Sekine, S. Kimura, N. Hamaya, J. Solid State Chem. 142 (1999) 146.
[6] I. Shirotani, T. Uchiumi, K. Ohno, C. Sekine, Y. Nakazawa, K. Kanoda, S. Todo, T. Yagi, Phys. Rev. B 56 (1997) 7866.
[7] T. Uchiumi, I. Shirotani, C. Sekine, S. Todo, T. Yagi, Y. Nakazawa, K. Kanoda, J. Phys. Chem. Solids 60 (1999) 689.
[8] E.D. Bauer, N.A. Frederick, P.-C. Ho, V.S. Zapf, M.B. Maple, Phys. Rev. B 65 (2002) 100506R.
[9] M.S. Torikachvili, C. Rossel, M.W. McElfresh, M.B. Maple, R.P. Guertin, G. P. Meisner, J. Magn. Magn. Mater. 54 (1986) 365.
[10] M.E. Danebrock, C.B.H. Evers, W. Jeitschko, J. Phys. Chem. Solids 57 (1996) 381.
[11] L. Keller, P. Fischer, T. Herrmannsdörfer, A. Dönni, H. Sugawara, T.D. Matsuda, K. Abe, Y. Aoki, H. Sato, J. Alloy. Compd. 323 (2001) 516.
[12] K. Tenya, N. Oeschler, P. Gegenwart, F. Steglich, N.A. Frederick, E.D. Bauer, M. B. Maple, Acta Physica Pol. B 34 (2003) 995.
[13] C. Sekine, T. Uchiumi, I. Shirotani, K. Matsuhira, T. Sakakibara, T. Goto, T. Yagi, Phys. Rev. B 62 (2000) 11581.
[14] C. Sekine, T. Uchiumi, I. Shirotani, T. Yagi, Phys. Rev. Lett. 79 (1997) 3218.
[15] S.V. Dordevic, D.N. Basov, N.R. Dilley, E.D. Bauer, M.B. Maple, Phys. Rev. Lett. 86 (2001) 684.
[16] A. Yamasaki, S. Imada, T. Masuda, T. Nanba, A. Sekiyama, H. Sugawara, T. D. Matsuda, H. Sato, C. Sekine, I. Shirotani, H. Harima, S. Suga, Acta Physica Pol. B 34 (2003) 1035.
[17] E.D. Bauer, A. Slebarski, E.J. Freeman, C. Sirvent, M.B. Maple, J. Phys.: Condens. Matter 13 (2001) 4495.
[18] B.C. Sales, in: J.-C. Bunzil K.A. Gschneider (Eds.), Handbook on the Physics and Chemistry of Rare-earths, 33, 2003, Amsterdam, Netherlands, Elsevier.
[19] G.S. Nolas, D.T. Morelli, T.M. Tritt, Annu. Rev. Mater. Sci. 29 (1999) 89.
[20] J.J. Pulikkotil, H.N. Alshareef, U. Schwingenschlögl, Chem. Phys. Lett. 514 (2011) 54–57.
[21] F. Grandjean, A. Gérard, D.J. Braun, W. Jeitschko, J. Phys. Chem. Solids 45 (1984) 877.
[22] W. Jeitschko, D.J. Braun, Acta Crystallogr. 33 (1977) 3401.
[23] Hisatomo Harima, Katsuhiko Takegahara, Physica B 328 (2003) 26–28.
[24] Katsuhiko Takegahara, Hisatomo Harima, J. Magn. Magn. Mater. 310 (2007) 861–863.
[25] M. Hachemaoui, R. Khenata, A. Bouhemadou, S. Bin-Omran, Ali H. Reshak, F. Semari, D. Rached, Solid State Commun. 150 (2010) 18691873.
[26] K. Nouneh, Ali H. Reshak, S. Auluck, I.V. Kityk, R. Viennois, S. Benet, S. Charar, J. Alloy. Compd. 437 (2007) 39–46.
[27] A.H. Reshak, M. Piasecki, S. Auluck, I.V. Kityk, R. Khenata, B. Andriyevsky, C. Cobet, N. Esser, A. Majchrowski, O.M. S wirkowicz, R. Diduszko, W. Szyrski, J. Phys. Chem. B 113 (2009) 15237–15242.
[28] F. Tran, P. Blaha, Phys. Rev. Lett. 102 (2009) 226401.
[29] Y. Saeed, S. Nazir, A. Shaukat, A.H. Reshak, J. Magn. Magn. Mater. 322 (2010) 3214–3222.
[30] Mohammed BenaliKanoun, AliH. Reshak, Nawel Kanoun-Bouayed, Souraya Goumri-Said, J. Magn. Magn. Mater. 324 (2012) 1397–1405.
[31] Hardev S. Saini, Singh Mukhtiyar, A.H. Reshak, Manish K. Kashyap, J. Magn. Magn. Mater. 331 (2013) 1–6.
[32] A.H. Reshak, Sikander Azam, Z.A. Alahmed, Jan Chyský, J. Magn. Magn. Mater. 351 (2014) 98–103.
[33] A.H. Reshak, H. Kamarudin, Z.A. Alahmed, S. Auluck, Jan Chyský, J. Magn. Magn. Mater. 361 (2014) 206–211.
[34] P. Blaha, K. Schwarz, G.K.H. Madsen, D. Kvasnicka, J. Luitz, WIEN2k: An Augmented Plane Wave Plus Local Orbitals Program for Calculating Crystal Properties, Vienna University of Technology, Austria, 2001.
[35] J.P. Perdew, A. Zunger, Phys. Rev. B 23 (1981) 5048.
[36] T. Kamagai, Y. Nakanishi, H. Sugawara, H. Sato, M. Yoshizawa, Physica B 329 (2003) 471.
[37] Y. Nakanishi, T.D. Matsuda, H. Sugawara, H. Sato, M. Yoshizawa, Physica B 312 (2002) 827.
[38] C. Recknagel, N. Reinfried, P. HÖhn, W. Schnelle, H. Rosner, Yu Grin, A. Leithe-Jasper, Sci. Technol. Adv. Mater. 8 (2007) 357.